

Influence of Resonator Material on the Performance of Thermoacoustic Refrigerator

Ramesh Nayak. B

Associate Professor, Department of Industrial Engineering and Management,
B.M.S. College of Engineering, Bengaluru – 560019, Karnataka, India,

Abstract: The work reported in this paper is focused on the performance of a thermoacoustic refrigerator under various operating conditions. The experiments were conducted with different resonator materials like Aluminium and PVC. Stack having parallel plates of Mylar material with 0.12mm thick spaced with 0.36mm. Aluminium resonator coated with polyurethane material from inside to reduce conduction heat losses. Helium gas was used as a working fluid. The experiments were also conducted with different drive ratio ranging from 1.5 to 2.5% with varying heating load from 2W to 10W. During the experiments operating frequencies from 200Hz to 600Hz with mean pressure varying from 2 bar to 10 bar in steps of 2 bar each were considered. The temperatures of the hot and cold end of the heat exchangers are recorded using RTDs and data acquisition system under various operating conditions. The COP and relative COP (COPR) are evaluated. Results shows that COP of the refrigerator increases with increase of heating load. It was also observed that the temperature difference between hot end and cold end of the stack is higher at 2W heating load for 400Hz operating frequency. The temperature difference between the hot end and cold end of the stack and COP was observed to be 10 % more for PVC resonator compared to Aluminium resonator due to negligible heat loss from the resonator tube for 10 bar mean pressure and 2W heating load at 2.5% drive ratio.

Keywords: Aluminium Resonator, PVC Resonator, Helium gas, COP and COPR,

Date of Submission: 06-02-2023

Date of Acceptance: 18-02-2023

I. INTRODUCTION

The discovery of thermoacoustic phenomenon goes back to more than a century ago, but the significant work in this area was started about two decades ago at the Los Alamos National Laboratory by the research group of Greg Swift. They have developed different types of thermoacoustic refrigerators and heat engines [1]. George Mozurkewich studied heat transport in a resonator tube. Heat transfer coefficient is proportional to the square root of amplitude for a long object. The magnitude of heat transfer from the heated wall segment is increased by inserting an object into the tube. In the empty resonator tube the localized streaming velocity is greater than the global streaming velocity. This effect is used to cool the electronic components and thermoacoustic engines [2]. P. Nika., et al. studied the regenerator of a Stirling engine filled with stack of beds in a cylindrical envelop using linear thermoacoustic theory. They calculated the temperature amplitude, velocity and pressure and proposed the regenerator to formulate the thermal time constant. A global equivalent electrical scheme of the regenerator is deduced. The total axial energy flux expression is established. The influence of the thermal time constant and various impedance was discussed in this paper [3]. Tang et al., simulated thermoacoustic engine using linear thermoacoustic equations and studied the influence of resonator length on the performance of thermoacoustic engine and pulse tube refrigerator. Theoretical results were compared with the experimental results. A refrigeration temperature of 88.6 K has been obtained at 8 m optimized length of the resonator tube using helium as working substance and 2200W of heating power. Temperature difference of 19.6 K was achieved with varying resonator tube from 4 m to 8 m [4]. Amjad et al., designed and developed thermoacoustic refrigerator with an adjustable mechanical resonator attached to the acoustic resonator. Mechanical resonator with the acoustical resonator of the thermoacoustic system is coupled to get the better efficiency from the refrigerator. The maximum efficiency obtained by matching the mechanical and acoustical resonator frequencies. Experimental results show 10% improved efficiency of the refrigeration compared with thermoacoustic refrigerator with no mechanical resonator [5]. An oil-heated thermoacoustic refrigerator was constructed in order to investigate the use of waste-heat sources to operate a refrigerator. Fluid flows within the resonator in the vicinity of the stack and heat exchanger assemblies were measured through optical means. During the course of the experiment, anomalous centerline steady flows were observed at magnitudes of up to three times the acoustic amplitudes within the resonator of the thermoacoustic device. An evanescent component

of the acoustic field was also measured at the same location. An order of magnitude calculation indicates that the body force induced by the evanescent mode is of sufficient magnitude and structure to source the streaming [6]. A novel Helmholtz resonator is proposed to focus acoustic energy of a TE to its load. In fact, the proposed Helmholtz resonator is a variation of traditional Helmholtz resonator. Influenced by the compliance impedance of the reservoir, the resonator tube shows different transmission characteristics from the acoustic amplifiers. A Helmholtz resonator can get maximal pressure amplitude with different lengths, which is determined by the matching between the resonator tube and reservoir. As is shown in computations and experiments, the Helmholtz resonator shows remarkable amplifying ability of pressure amplitude. As is shown by computations, the acoustic power transmission ability of Helmholtz resonator is strong. When the Helmholtz resonator is in resonance state, it has large volume flow rate at both the resonator tube ends. The outlet volume flow rate and the outlet pressure amplitude peak at the same position. The transmission characteristics of the Helmholtz resonator indicate that it may also be used to tune the interior acoustic field of a TE [7]. B. Wang et al., derived a passive network model based on fluid network theory in order to calculate passive tube systems and make linear thermoacoustic theory coincide closely with experimental results. This method is proposed to correct turbulence by modifying thermal and viscous penetration depths when the ratio of the tube radius to the viscous penetration depth is large. The experiments are conducted to verify the model in the acoustic amplifier, Helmholtz resonator, and inertance tube [8]. This paper presents a study of the impact of the resonance tube on performance of a thermoacoustic stack. The resonance tube is a key component of a standing-wave thermoacoustic refrigerator. The appropriated resonance tube's length leads to an increase of performance of the stack in terms of the temperature difference. The results also indicate that the optimal operating frequency differs from the design based on the equation of a half-wavelength. The resonance tube length is elongated to compensate for some effects that occur in the resonance tube, especially when the stack is placed in the resonance tube. The relationship of these parameters is necessary to the design and measurement performance of the thermoacoustic refrigeration system [9]. In this study, the theoretical and experimental investigations are carried out to examine the influence of PT, PS, and resonator length with constant stack length on the performance of standing wave open end thermoacoustic prime mover. Experiments are conducted to observe the system performance in terms of onset temperature difference frequency, and pressure amplitude. The experimental results showed that the PT of 0.3 mm yielded a large onset temperature difference to generate oscillations when compared to 0.5 mm plates irrespective of PS. Increase in PS and resonator length leads to decrease in working frequency and increase in onset temperature difference and pressure amplitude for both 0.3 mm and 0.5 mm thick plates. Also, the normalized acoustic power generated from the 0.3 mm PS is higher than the 0.5 mm. This acoustic power decreases with increase in resonator length and decrease in plate thickness. In the present system, 230–250 Hz frequency of acoustic waves is generated which may be adequate to drive a thermoacoustic refrigerator. The theoretical results obtained from DeltaEc are in good agreement with the experimental results [10]. Study the performance of the thermoacoustic refrigerator with respect to various operating conditions and different stack geometries using air and helium as the working medium. The factors that influence the performance of the system were identified. The temperature difference (ΔT) between hot end and cold end of the stack is higher at 2W heating load for 400Hz operating frequency with a mean pressure of 10 bar [11-13].

II. EXPERIMENTAL SETUP

Thermoacoustic refrigerator is designed for a cooling power of 10W considering pure Helium and compressed air as the working medium. The design of various components such as Stack, different stack geometry, variable pressure, resonator tube, heat exchangers and buffer volume has been carried out with the help of relevant thermoacoustic equations.

Figure 1 shows the schematic layout of the thermoacoustic refrigerator. The main parts of thermoacoustic refrigerator consists of acoustic driver, two heat exchangers, stack which acts as a heat pumping element and the resonator system. Figure 2 shows the Experimental setup of the Aluminium Resonator Thermoacoustic Refrigerator and Figure 3 shows the Experimental setup of the PVC Resonator Thermoacoustic Refrigerator.

The thermoacoustic refrigerator is designed and optimized for a quarter wave length resonator. A cone shape buffer volume is accommodated in order to simulate open end condition. The resonator system consists of large diameter tube and small diameter tube. The entire resonator system was constructed from aluminium. The inner surface of the resonator tube was coated with polyurethane material to reduce conduction heat loss. The stack having parallel plates constructed of 0.12mm thick Mylar sheets spaced with 0.36mm apart shown in figure 4. Copper tube type heat exchangers were employed at two ends of the stacks. The entire thermoacoustic system was made leak proof and tested for a pressure up to 20bar.

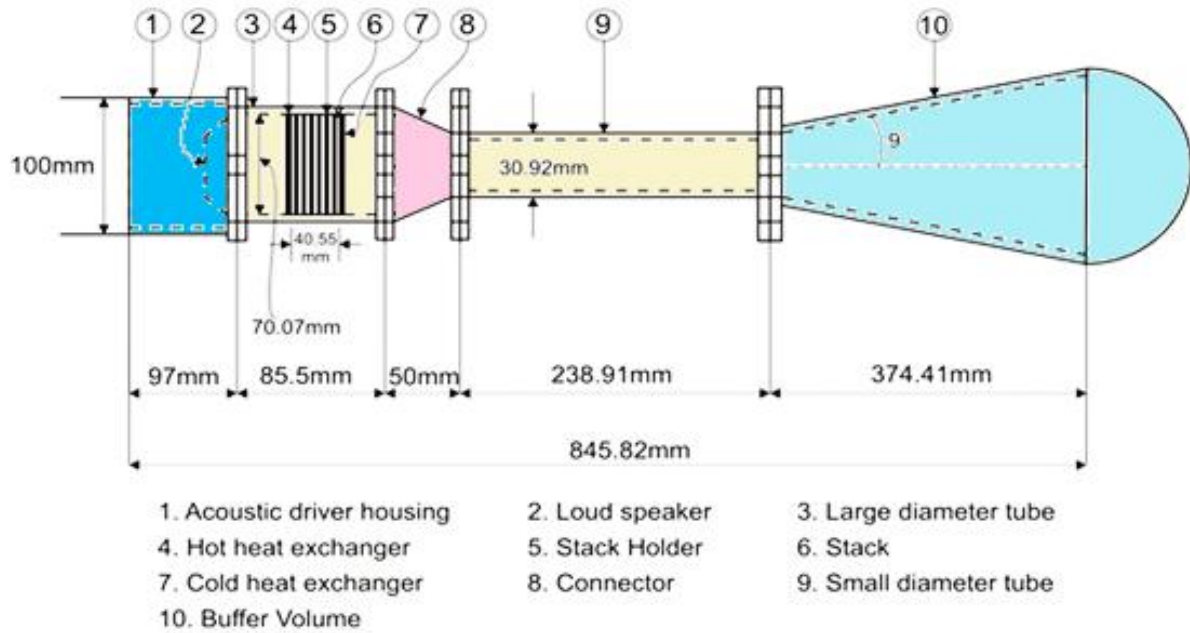


Figure 1: Schematic diagram of a standing-wave thermoacoustic refrigerator

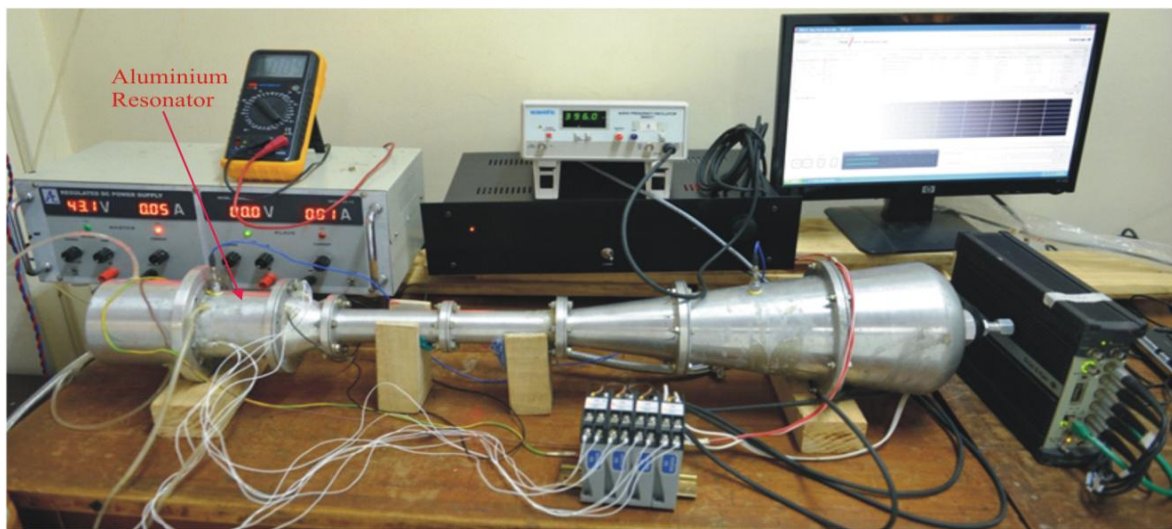


Figure 2: Experimental setup of the Aluminium Resonator Thermoacoustic Refrigerator

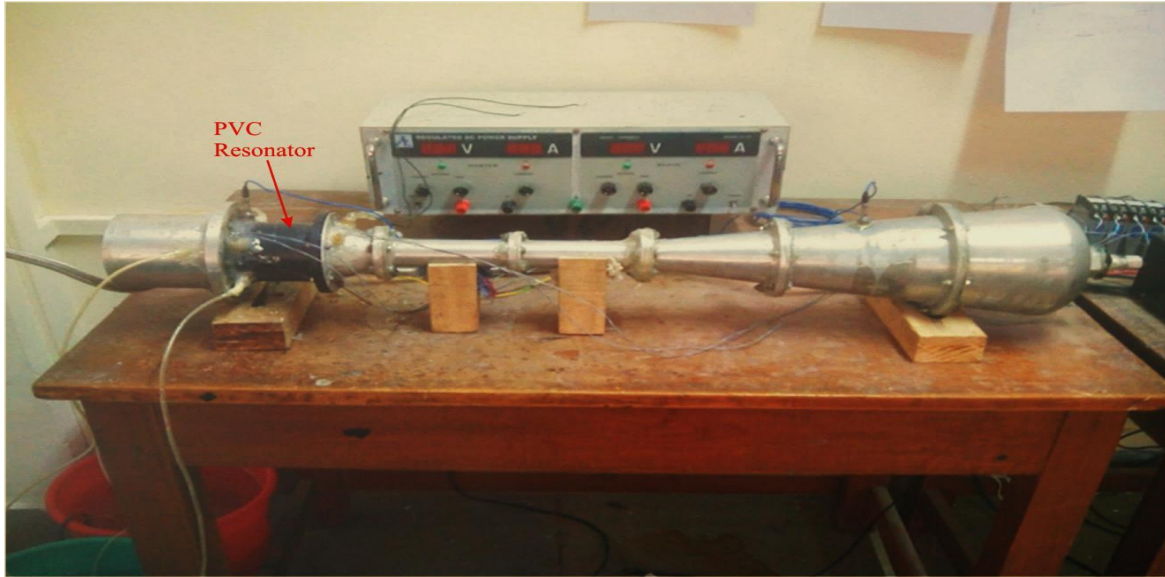


Figure 3: Experimental setup of the PVC Resonator Thermoacoustic Refrigerator



Figure 4: Parallel plates Stack

III. EXPERIMENTAL PROCEDURE

The experiments were conducted to evaluate the performance of the thermoacoustic refrigeration system under various operating conditions with different resonator materials. The resonator tube was filled with Helium gas with the help of regulating systems. The initial mean pressure was varied from 2 bar to 10 bar in steps of 2 bar. The desired frequency was set and then increased slowly from 200 Hz to 600 Hz in steps of 100 Hz for each trial. The heating load was controlled using resistance heating coil placed on the cold heat exchanger. The experimental data were recorded for each trial after the system is stabilized. The experiments were conducted by varying frequency, heating load and mean pressure for each set of experiments. The experiments were repeated for different input power to the acoustic driver thereby maintaining desired drive ratio. Cooling arrangements for acoustic driver and hot heat exchanger were made to remove heat generated in the refrigerator system.

IV. RESULTS AND DISCUSSIONS

The thermal performance of a thermoacoustic refrigerator subjected to various operating conditions such as frequency, mean pressure, acoustic input power, heating load and different resonators are discussed.

The performance of the thermoacoustic refrigerator is evaluated using performance parameters such as the cooling power, acoustic input power and temperature difference for various operating conditions. The

electric power introduced into the system is converted into acoustic power in the acoustic driver. The coefficient of performance (COP) is the ratio of heating load to the acoustic input power. The Carnot COP (COP_C) is calculated as the ratio of cold end temperature to the temperature difference of hot and cold ends as $[T_C / (T_H - T_C)]$. COPR is the ratio of the actual COP to COP_C and is often used to measure the performance of refrigerators.

4.1 Frequency (F)

The variation of temperature difference with frequencies at constant mean pressure and heating load is shown in Figures 5 - 16 shows the effect of frequency on the temperature. It is evident from the figures that the frequency increases with increase in temperature difference across the stack. The temperature difference reaches maximum at 400 Hz. This variation is due to the sound energy present in the PVC resonator is more compared to Aluminium resonator tube. This clearly shows the relation between operating frequency and natural resonance frequency of refrigerator which is responsible for change in the temperature difference across the hot and cold ends of the stack. The magnitude of the temperature difference between the hot end and the cold end of the stack increases with increase in mean pressure and maximum temperature difference was found for heating load of 2W corresponding to a mean pressure of 10 bar for both PVC and Aluminium resonators. The temperature difference between the hot end and cold end of the stack was observed to be 10 % more for PVC resonator compared to Aluminium resonator due to negligible heat loss from the resonator tube for 10 bar mean pressure and 2W heating load at 2.5% drive ratio.

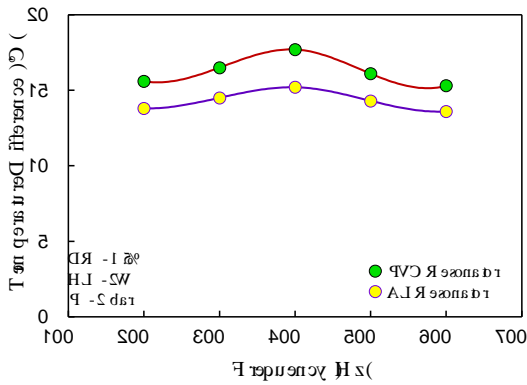


Figure 5: Variation of ΔT with Frequency for 2 bar pressure, 2W heating load and 1.5% DR

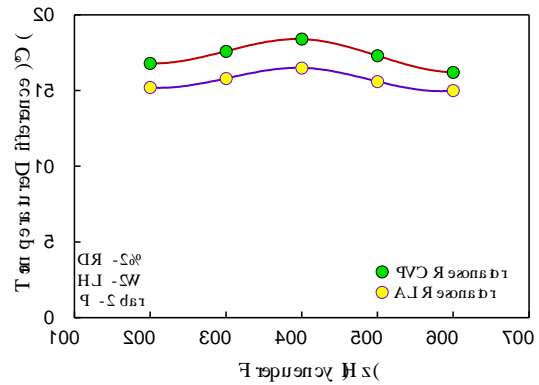


Figure 6: Variation of ΔT with Frequency for 2 bar pressure, 2W heating load and 2% DR

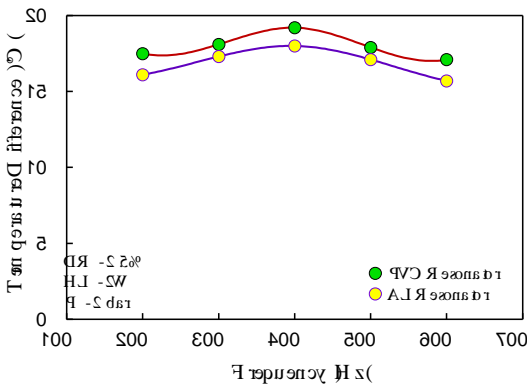


Figure 7: Variation of ΔT with Frequency for 2 bar pressure, 2W heating load and 2.5% DR

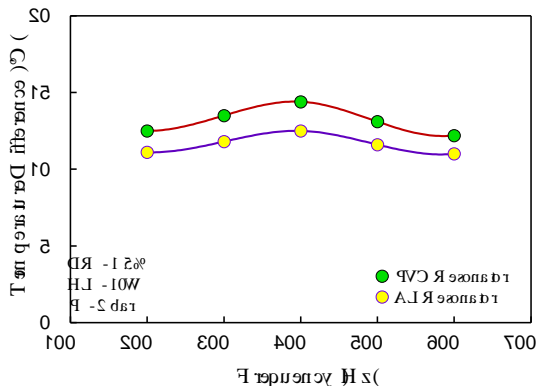


Figure 8: Variation of ΔT with Frequency for 2 bar pressure, 10W heating load and 1.5% DR

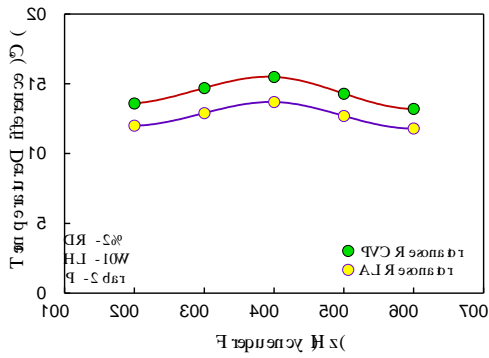


Figure 9: Variation of ΔT with Frequency for 2 bar pressure, 10W heating load and 2% DR

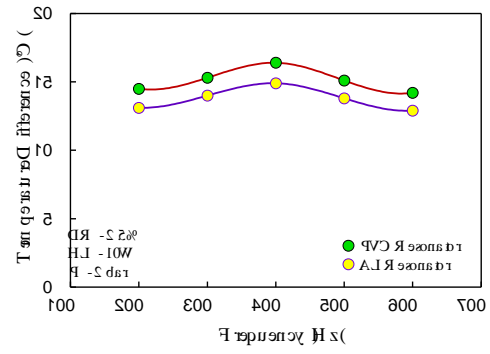


Figure 10: Variation of ΔT with Frequency for 2 bar pressure, 10W heating load and 2.5% DR

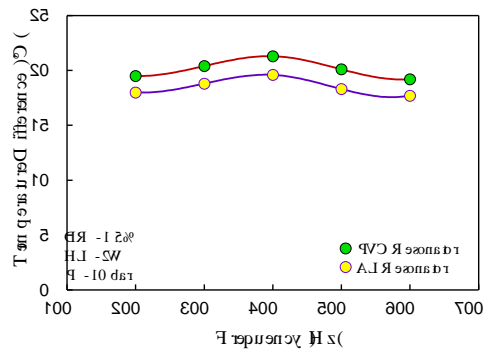


Figure 11: Variation of ΔT with Frequency for 10 bar pressure, 2W heating load and 1.5% DR

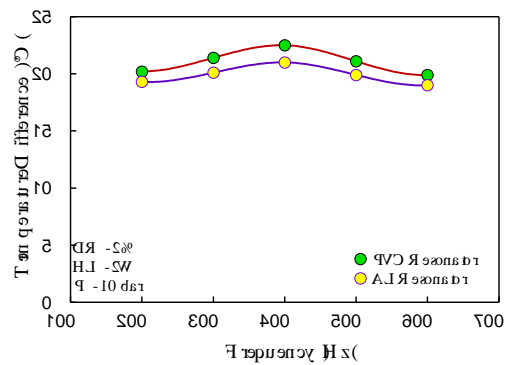


Figure 12: Variation of ΔT with Frequency for 10 bar pressure, 2W heating load and 2% DR

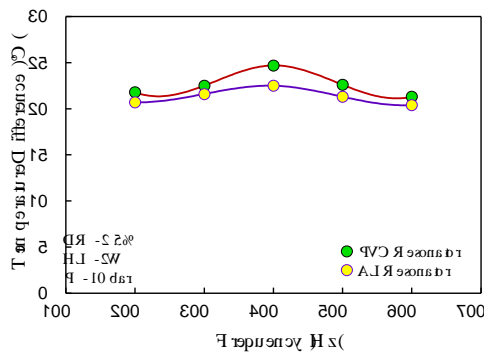


Figure 13: Variation of ΔT with Frequency for 10 bar pressure, 2W heating load and 2.5% DR

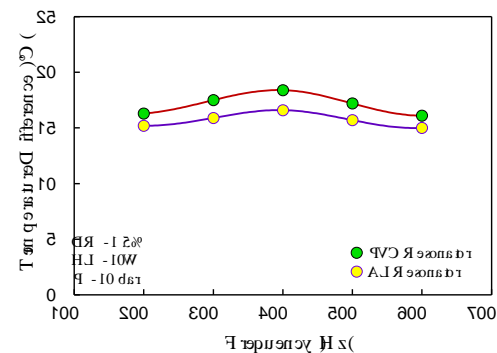


Figure 14: Variation of ΔT with Frequency for 10 bar pressure, 10W heating load and 1.5% DR

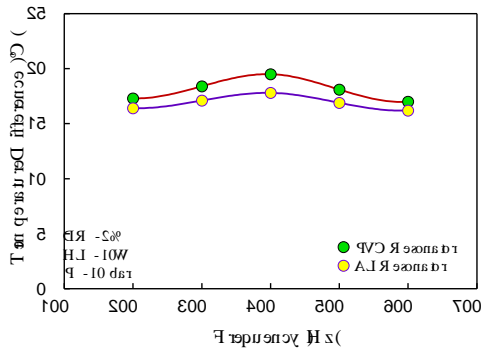


Figure 15: Variation of ΔT with Frequency for 10 bar pressure, 10W heating load and 2% DR

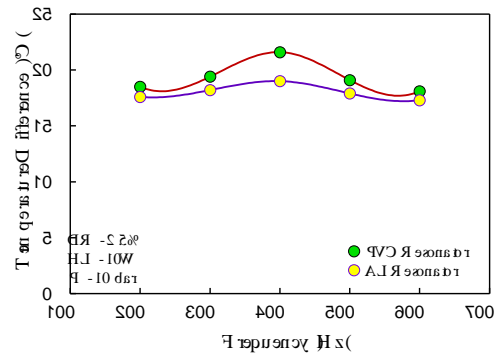


Figure 16: Variation of ΔT with Frequency for 10 bar pressure, 10W heating load and 2.5% DR

4.2 Heating Load (HL)

Figures 17 - 22 represent the variation of temperature difference with heating load for constant mean pressure and frequency. Temperature difference is a function of the heating load. Higher temperatures are achieved with higher dynamic pressure. Measurements are made using three drive ratios for parallel plate stack with helium as the working fluid. Figures show that the temperature difference is maximum corresponding to a heating load of 2W. This variation is due to the fact that the acoustic power input available is sufficient to remove the heat generated at cold end of the stack for PVC resonator compared to Aluminium resonator and for higher heating loads it is not sufficient for all pressures due to the very low electroacoustic energy conversion efficiency of the acoustic driver. It is also evident from figures that the temperature difference between hot end and cold end of stack is found to be more for PVC resonator compared to Aluminium resonator for the same operating conditions.

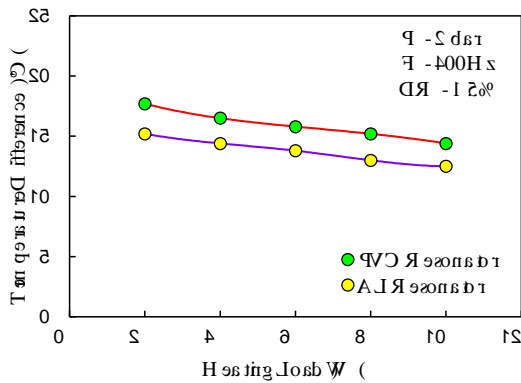


Figure 17: Variation of ΔT with heating load for 2 bar pressure, 400 Hz Frequency and 1.5% DR

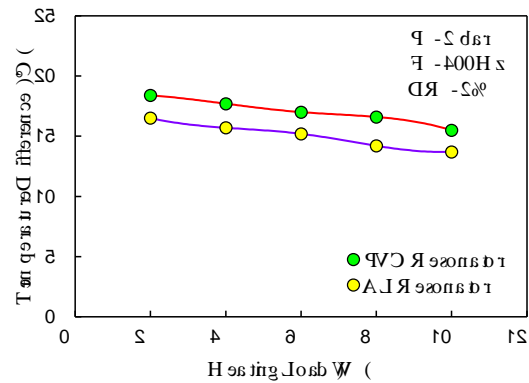


Figure 18: Variation of ΔT with heating load for 2 bar pressure, 400 Hz Frequency and 2% DR

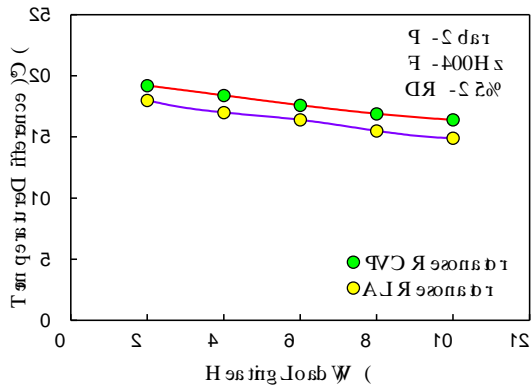


Figure 19: Variation of ΔT with heating load for 2 bar pressure, 400 Hz Frequency and 2.5% DR

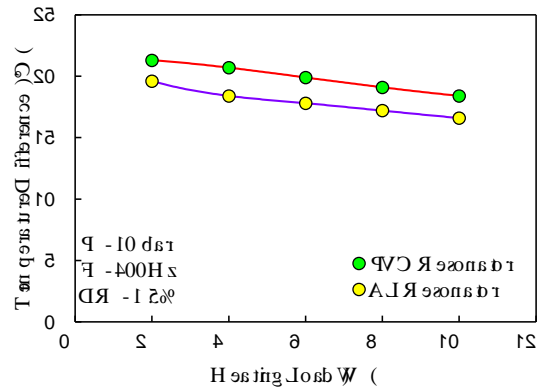


Figure 20: Variation of ΔT with heating load for 10 bar pressure, 400 Hz Frequency and 1.5% DR

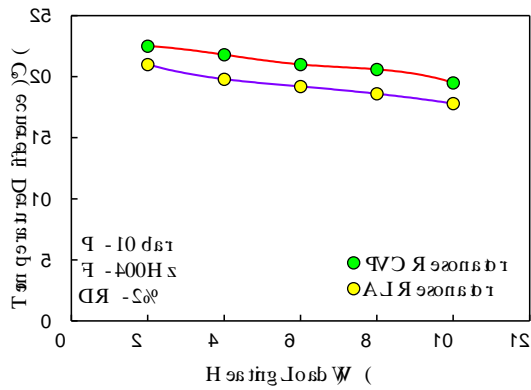


Figure 21: Variation of ΔT with heating load for 10 bar pressure, 400 Hz Frequency and 2% DR

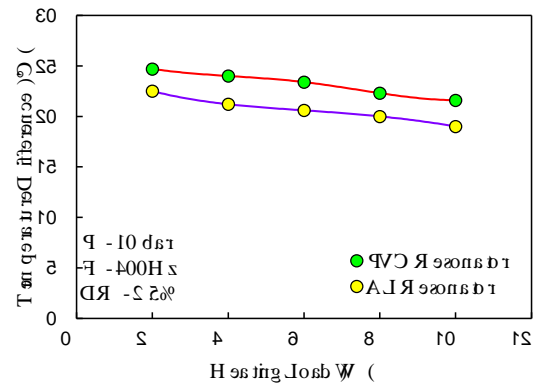


Figure 22: Variation of ΔT with heating load for 10 bar pressure, 400 Hz Frequency and 2.5% DR

4.3 Coefficient of Performance (COP)

Figure 23 shows the variation of COP with heating load for different drive ratios. COP increases with the increase in heating load as it is directly proportional to heating load. It is found that COP increases with decrease in drive ratio due to increase in acoustic power input. COP of the PVC resonator is found to be more efficient compared to Aluminium resonator because of its effective thermal penetration depth leading to efficient heat removal from the cold end of the stack shown in Figure 24.

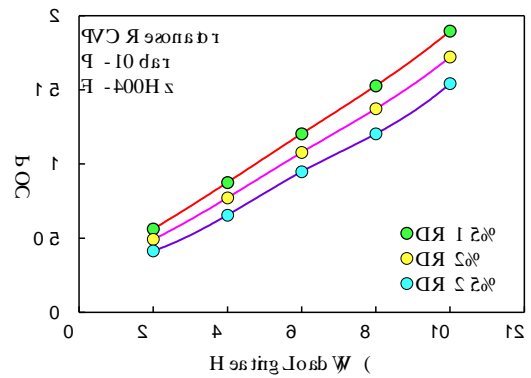


Figure 23: Variation of COP with heating load at 10 bar pressure and 400 Hz frequency for PVC

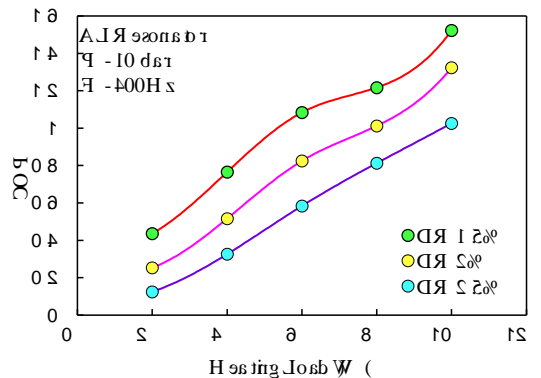


Figure 24: Variation of COP with heating load at 10 bar pressure and 400 Hz frequency for AL

resonator

resonator

4.4 Relative Coefficient of Performance (COPR)

Figures 25 – 36 shows the variations of COPR with frequency for different resonator materials shown therein for helium as the working fluid. It can be seen from these figures that the COPR is maximum for PVC resonator compared to Aluminium resonator. This phenomenon shows the importance of the thermal and viscous penetration depth on the performance of the thermoacoustic refrigerator. The COPR increases with the increase in COP as it is proportional to the COP and is found maximum at 400 Hz frequency corresponding to a mean pressure of 10 bar and 10W Heating Load for PVC resonator at drive ratio 1.5%. This is due to the presence of weak thermal penetration depth in the stack at higher operating frequencies leading to the increase in viscous loss and reducing the thermoacoustic effect.

The COPR is also increases with increase in heating load as it is directly proportional to the COP as shown in Figs. 19 and 20 for mean pressure of 2 bar and 10 bar respectively. The COPR increases with the mean pressure as it is proportional to thermoacoustic heat pumping power. The COPR increases with the mean pressure and approaches its maximum limit. Hence, the effect of mean pressure and other operating conditions could be different for systems operating with high drive ratios. Negligible energy losses taking place in the PVC resonator compared to Aluminium resonator at high velocity regions.

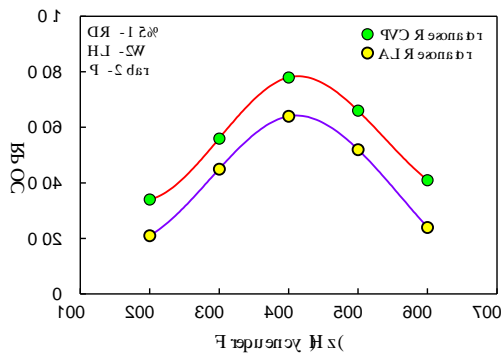


Figure 25: Variation of COPR with Frequency for 2 bar pressure, 2W heating load and 1.5% DR

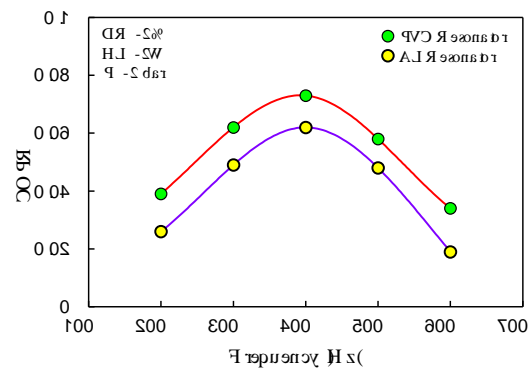


Figure 26: Variation of COPR with Frequency for 2 bar pressure, 2W heating load and 2% DR

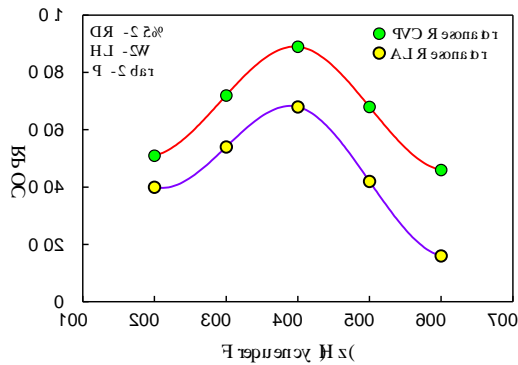


Figure 27: Variation of COPR with Frequency for 2 bar pressure, 2W heating load and 2.5% DR

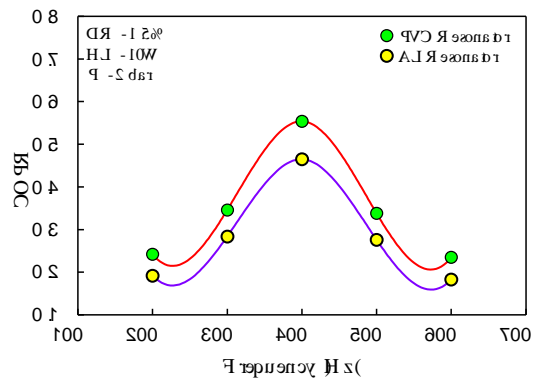


Figure 28: Variation of COPR with Frequency for 2 bar pressure, 10W heating load and 1.5% DR

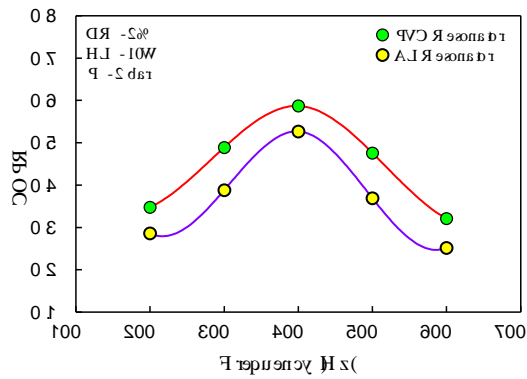


Figure 29: Variation of COPR with Frequency for 2 bar pressure, 10W heating load and 2% DR

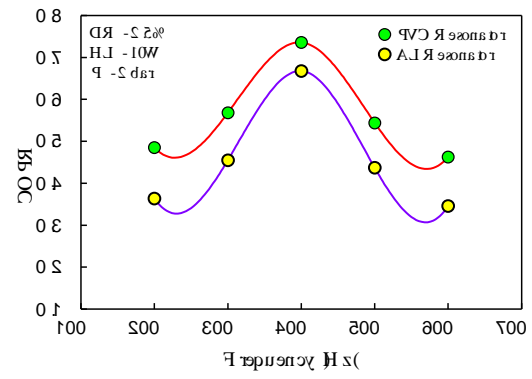


Figure 30: Variation of COPR with Frequency for 2 bar pressure, 10W heating load and 2.5% DR

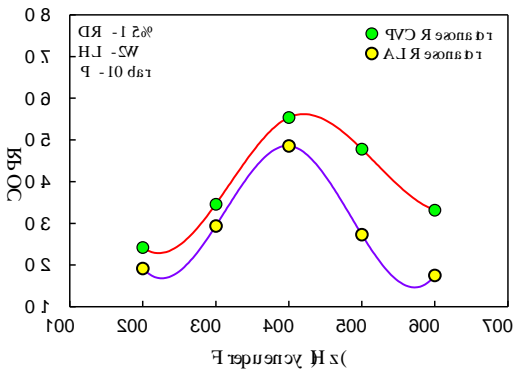


Figure 31: Variation of COPR with Frequency for 10 bar pressure, 2W heating load and 1.5% DR

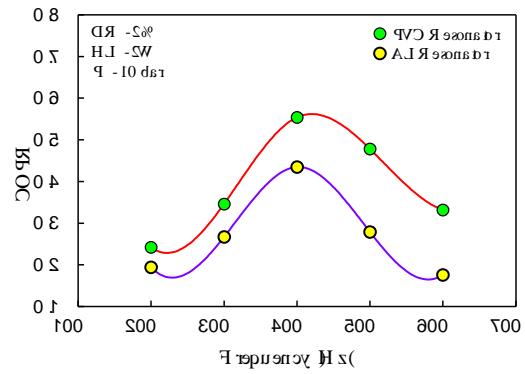


Figure 32: Variation of COPR with Frequency for 10 bar pressure, 2W heating load and 2% DR

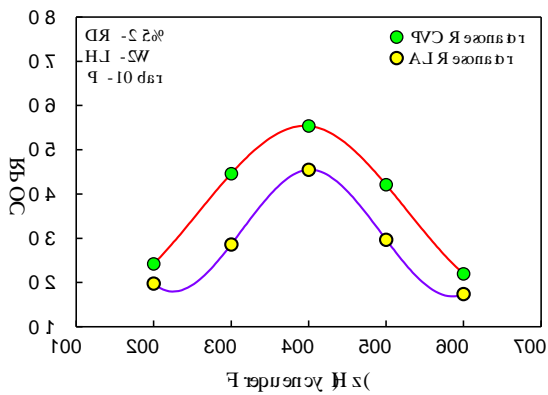


Figure 33: Variation of COPR with Frequency for 10 bar pressure, 2W heating load and 2.5% DR

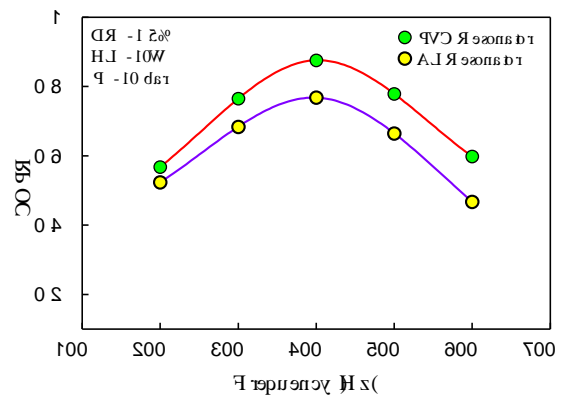


Figure 34: Variation of COPR with Frequency for 10 bar pressure, 10W heating load and 1.5% DR

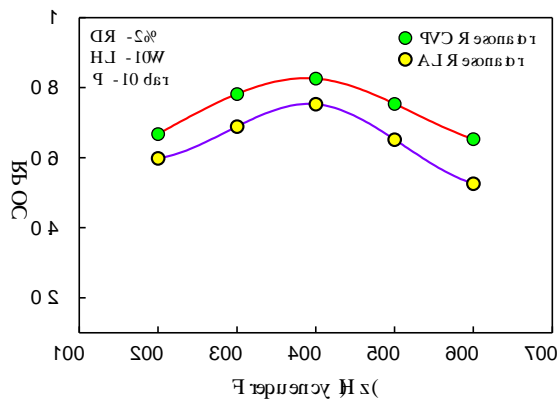


Figure 35: Variation of COPR with Frequency for 10 bar pressure, 10W heating load and 2% DR

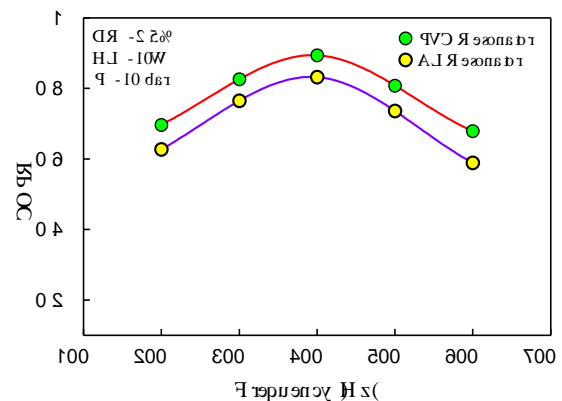


Figure 36: Variation of COPR with Frequency for 10 bar pressure, 10W heating load and 2.5% DR

V. Conclusions

Experimental study has been carried out in order to investigate the influence of resonator material on the behavior of thermoacoustic refrigerator under various operating conditions.

The influence of resonator material on the performance of the refrigerator is studied. The experimental results indicate that the stack performance of PVC resonator is better compared to Aluminium resonator in terms of heating power.

The maximum temperature difference of PVC resonator is 10% more compared to Aluminium resonator when helium is used as the working medium for 10 bar mean pressure corresponding to a heating load of 2W at 400 Hz frequency with drive ratio of 2.5%.

The highest COP were achieved for PVC resonator compared to Aluminium resonator with parallel plate stack when helium is used as the working medium for 10 bar mean pressure corresponding to a heating load of 10W at 400 Hz frequency with drive ratio of 1.5%.

References

- [1]. Swift S.W., Thermoacoustic engines and refrigerators, Physics Today, 48 (7), 1995, PP 22-28.
- [2]. George Mozurkewich, Heat transport by acoustic streaming within a cylindrical resonator, Applied Acoustics, 63, 2002, PP 713-735.
- [3]. P. Nika., M. Feidt, M.X. Francois, Y. Bailly, F. Lanzetta, Thermoacoustical effects in a cylindrical regenerator filled with a stack of beads, International Journal of Refrigeration 27, 2004, PP 150-164.
- [4]. K. Tang, G.B. Chen, T. Jin, R. Bao, B. Kong, L.M. Qiu, Influence of resonance tube length on performance of thermoacoustically driven pulse tube refrigerator, Cryogenics 45, 2005, PP 185-191.
- [5]. A. Amjadi., M. R. Abolhassani and S. Basir Jafari, Acousto-Refrigerator with an Adjustable Mechanical Resonator, IJE Transactions B: Applications Vol. 21, No. 2, August 2008, PP 183-196.
- [6]. Evanescence modes and anomalous streaming in a thermoacoustic device, Gordon P. Smith, Richard Raspet, Robert Hiller, Joseph McDaniel, Applied Acoustics 69, 2008, PP 23-30.
- [7]. Daming Sun, Limin Qiu, Bo Wang, Yong Xiao, Novel Helmholtz resonator used to focus acoustic energy of thermoacoustic engine, Applied Thermal Engineering, 29, 2009, PP 945-949.
- [8]. B. Wang, L.M. Qiu, D.M. Sun, K. Bai, T. Steiner, A passive network model for large diameter thermoacoustic tube systems and its experimental verification, Applied Acoustics, 71, 2010, PP 922-930.
- [9]. Channarong Wantha, Kriengkrai Assawamartbunlue, The Impact of the Resonance Tube on Performance of a Thermoacoustic Stack, Frontiers in Heat and Mass Transfer (FHMT), 2, 2011, PP 1-8.
- [10]. N.M. Harihara, P. Sivashanmugam, S. Kasthurirengan, Influence of stack geometry and resonator length on the performance of thermoacoustic engine, Applied Acoustics 73, 2012, PP 1052-1058.
- [11]. Ramesh Nayak. B., Bheemsha, Pundarika. G., "Performance Evaluation of Thermoacoustic Refrigerator Using Air as Working Medium", SSRG International Journal of Thermal Engineering (SSRG-IJTE), Volume 1, Issue 3, 2015, PP1-7.
- [12]. B Ramesh Nayak., G Pundarika., Bheemsha Arya., "Influence of stack geometry on the performance of Thermoacoustic Refrigerator", Sadhana, Indian Academy of Sciences, Volume 42, Issue 2, 2017, PP 223-230.
- [13]. Ramesh Nayak B., Pundarika G., "Comparison of Experimental and DELTA-EC Results on performance of Thermoacoustic Refrigerator", International Research Journal of Engineering and Technology (IRJET), Volume 09, Issue 06, 2022, PP 1894-1900.